Draft version May 6, 2023
Typeset using LaTeX **twocolumn** style in AASTeX631

Average Halo Specific Angular Momentum of MW, M31, and their Merger Remnant

Ritvik Basant [1]

[1] *Steward Observatory and Department of Astronomy, The University of Arizona, Tucson, AZ 85721, USA*

(Received 5^{th} May 2023)

ABSTRACT

Understanding how a galaxy's dark matter halo rotates – i.e., its spin – has been a field of extensive research. More importantly, exploring the spin of dark matter halo is not only crucial for understanding the evolution of the galaxy but for its formation as well. In this study, we analyze the average rotation of halos surrounding the MW, M31, and their merger remnant. Analyzing the halo spin evolution of MW – M31 is important not only because it hints at the final fate of our galaxy but also because it will help us understand various physical phenomena that drive the merger. We find that the merger remnant halo has a significantly higher spin than the initial halos of both galaxies. As the initial halos of both galaxies have negligible spin, our results indicate that the remnant halo is somehow gaining angular momentum quite efficiently. Understanding the mechanism behind how the remnant halo gains momentum will be important in understanding how the MW–M31 system evolves.

Keywords: Galaxy Merger, Merger Remnant, Major Merger, Dark Matter Halo, Halo Spin

1. INTRODUCTION

A bound collection of stars whose properties cannot be explained with Newton's laws of gravity and baryonic matter (i.e., visible matter) alone is known as a galaxy (Willman & Strader 2012). Therefore, to explain the gravitational forces observed in a galaxy, Fritz Zwicky proposed the existence of an invisible type of matter called Dark Matter (DM), whose first evidence came from his analysis of fast-moving galaxies in the Coma Cluster (Zwicky 1933). DM is decoupled from the expansion of the universe and arranges itself in the form of halos in which galaxies reside (Wechsler & Tinker 2018). Later, the analysis of the rotation curves of the M31 galaxy provided yet another piece of evidence for the existence of DM halos (Rubin & Ford 1970).

In the subsequent years, several studies were carried out and DM halos were identified as the breeding grounds for galaxies (see e.g., White & Rees 1978). Since then, the scientific community has aimed to constrain the properties of the DM halos (see e.g., Davis et al. 1985, analyze the triaxial shape of DM halos). If two galaxies come close enough such that they start interacting and cause significant disturbances to each other's stars and gas, the event is termed a galaxy merger (Lotz et al. 2011). The authors also define a major galaxy merger event as a merger where the mass ratio of both galaxies is less than 4:1. After the two interacting galaxies finally coalesce to form a single galaxy, the remaining product is termed a merger remnant.

It had been established very early, with the help of numerical simulations, that halos tend to rotate (Barnes & Efstathiou 1987). However, the exact strength of the spin and halo mass depends on the definition of the halo, with more massive halos appearing to spin slowly (Bett et al. 2007). The internal distribution of specific angular momentum inside a halo follows a rather simple trend, increasing with distance from the center (Frenk & White 2012). The alignment of the spin axis of halos with their three principal axes assumes a broad distribution (see e.g., Shaw et al. 2006; Bett et al. 2007). Additionally, the direction of angular momentum inside the halo varies with distance from the center (Bett et al. 2010).

Drakos et al. (2019) analyzed the merger remnant of two equal-massed halos (without baryons) with various density profiles. The authors find that the remnant halo may assume a complicated spin. Figure 1 shows how the spin of the remnant halo varies with the dimensionless energy parameter (K; tells the energy of the colliding halos) analyzed in Drakos et al. (2019). Abadi et al. (2010) examine the effects of the formation of a central galaxy on its surrounding halo. When the baryons were included, the authors found that both baryons and halo had comparable angular momenta initially, but baryons lost a significant amount of their angular momentum to the surrounding halo. Thus, in their simple model, the baryons moved inwards and their central galaxy was more massive and smaller. When Bett et al. (2010) included the effects of baryons, they find that the formation of a central galaxy increases the angular momentum of the halo significantly.

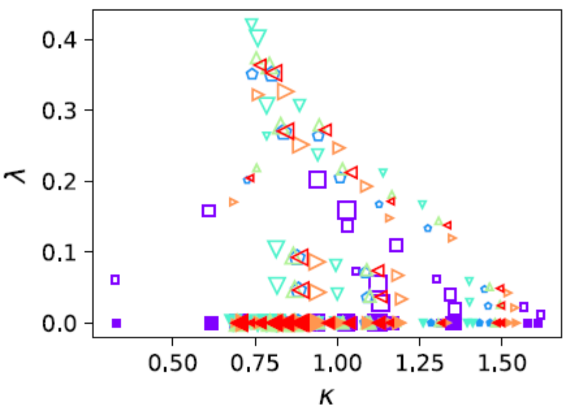

Figure 1. This figure has been adapted from Drakos et al. (2019). The x-axis shows the dimensionless energy parameter that describes the change in internal energy of the galaxy through a merger. The y-axis shows the dimensionless spin parameter that characterizes the rotation of the galaxy. For a more detailed explanation of the shapes and colors, we refer the readers to Drakos et al. (2019). $\kappa < 1$ signifies a less bound remnant, and therefore, has a higher spin as particles are far apart. On the other hand, $\kappa > 1$ represents a tightly bound remnant and has a low spin.

Rodriguez-Gomez et al. (2017) analyzed the effects of halo spin on galaxy morphology and found that for less massive halo mergers ($\lesssim 10^{10} M_{\odot}$), the halo spin plays a crucial role in determining the morphology of the galaxy while for halo masses comparable to that of the MW, the spin has weak effects on the morphology of the remnant. Thus, analyzing the evolution of halo spins through mergers is important to understand the evolution of galaxies, i.e., how the physical properties, structures, and morphology of galaxies change with time (Conselice 2014).

The halo spin parameter can be utilized to determine the angular momentum of embedded galaxies and, consequently, galaxy sizes (Fall & Efstathiou 1980). Furthermore, the halo spin parameter can be approximately described by a log-normal distribution (Bullock et al. 2001). However, an important question remains unanswered: What is the underlying mechanism behind the characteristic spin distribution, apart from random processes? Additionally, current studies (e.g., Drakos et al. 2019) often disregard the individual spin of the initial halos before the merger, possibly due to computational limitations. Another open question is how individual halo spins evolve through a major merger event. Even in simple models (such as that in Abadi et al. 2010), the inclusion of cold baryons (in the absence of star formation and feedback mechanisms) resulted in the formation of central galaxies that were significantly more massive. Therefore, the true effects of the inclusion of proper star formation and feedback mechanisms on the halo merger remnant are also unanswered.

2. THIS PROJECT

In this paper, we focus on another property of DM halos – their Average Specific Angular Momentum (ASAM). As M31 will soon collide with the Milky Way (MW) (Cox & Loeb 2008), in this paper, we want to study how the spin of individual galaxy halos (MW and M31) evolve through their merger by quantifying them at different points in time. We will begin by estimating the individual ASAM for the halos surrounding MW and M31 galaxies. We also estimate the time for periapsis approaches of both galaxies along with the time of the final merger.

Out of all the open questions we discussed in Section 1, this study aims to answer the following question: how does the halo spin of M31 and MW change through the merger? Moreover, if it changes significantly, which we believe it should, we try to find a reasonable mechanism responsible for this evolution.

In the context of MW and M31 – two galaxies bound to undergo a major merger – examining the ASAM becomes important due to three reasons: (i) First, the ASAM of individual galaxies can help us in testing the correlation between the halo spin and the size of the embedded galaxy (see e.g., Jiang et al. 2019) and the spin vs. morphology correlation, (ii) it gives us a way to assess how the merger remnant halo spin relates to the spin of the initial galaxies, and lastly, (iii) it can be used to examine how the DM spin evolves through a merger.

3. METHODOLOGY

In this paper, we rely heavily on the work of van der Marel et al. (2012), who performed detailed collisionless N-*body* simulation of the MW – M31 – M33 system using only stars and DM particles in these galaxies. In an N-*body* simulation of a galaxy, the whole galaxy is assumed to consist of N particles (which can range from a few hundred to millions) whose mass, velocities, and positions are tracked over time as they interact via Newton's gravitational laws. In simple words, N-*Body* simulation is when we use the gravitational laws iteratively on N bodies instead of just two. The N particles represent the stars, or a cluster of stars, and DM mass in the galaxy. Thus, N-*Body* simulations can help in predicting the fate of a system.

To calculate the ASAM of the galaxy halo at a given time, we first calculate the center of mass positions and velocities of the whole galaxy using the disk particles and the updated COM code we developed in Homework-6. Then we calculate the new positions and velocities of each halo particle in the simulation file relative to the center of mass. With these new positions and velocities, and mass - from the original simulation file - we calculate the total halo angular momentum of the galaxy using the equation $\vec{L} = m\vec{r} \times \vec{v}$, where m is the mass, $\vec{r}$ is position, and $\vec{v}$ is the velocity of a single halo particle. Finally, to calculate the ASAM, we iterate over all halo particles to calculate the total halo angular momentum and divide it by the total halo mass. The whole approach is schematically depicted in Figure 2.

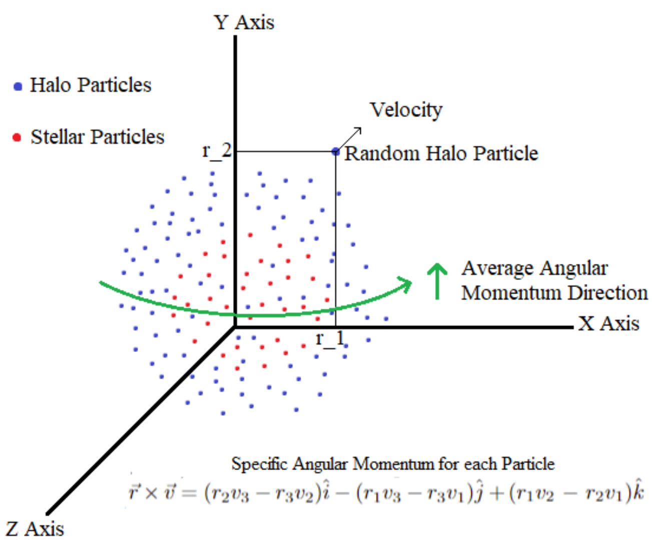

Figure 2. This figure shows galaxy halo and stellar particle distribution. We also show a random halo particle's velocity and x, y, and z coordinates (Note: z coordinate for the selected particle is 0 in this case). We also plot an example of the direction of the angular momentum of the whole body.

Recall that the specific angular momentum is a vector. Thus, to quantify the angular momentum correctly using Python, we have developed a new code that can calculate the net angular momentum vector, and therefore, the ASAM. The idea to do this is simple: for each halo particle, we have 3 velocities (x, y, and z) and three position coordinates (x, y, and z). The cross product of two vectors (say $\vec{r}$ and $\vec{v}$) in terms of their components can be written as in equation 1 (where m_i is the mass of i^{th} halo particle and r_j & v_j – j = 1 (x), 2 (y), 3 (z) – are the position and velocity coordinates). Thus, for each of the halo particles, we calculate its angular momentum using equation 1 and store the individual $\hat{i}, \hat{j}$, and $\hat{k}$ components separately. At last, we sum individual components over all the halo particles to estimate the total halo angular momentum in each direction. Dividing this quantity by the total halo mass yields the halo ASAM for the galaxy.

$$L_i = m_i \left[(r_2v_3 - r_3v_2)\hat{i} - (r_1v_3 - r_3v_1)\hat{j} + (r_1v_2 - r_2v_1)\hat{k}\right] \tag{1}$$

An important point to note here is that after both galaxies merge, their relative velocities are close to zero, i.e., the center of mass frame of one galaxy can be roughly assumed to be the same as that of the other one. Thus, with this assumption, the remnant halo ASAM can be calculated by adding both individual galaxies' spins after the merger. However, as the DM particle mass is different in MW and M31, we will add the ASAM of both galaxies in the ratio of their masses:

$$S_{rem.} = \frac{S_{MW} \times m_{DM,MW} + S_{MW} \times m_{DM,M31}}{m_{DM,MW} + m_{DM,M31}} \tag{2}$$

where S represents the ASAM, and $m_{DM,MW}$ and $m_{DM,M31}$ are the DM particle mass in MW and M31 galaxy respectively.

We also use the OrbitCOM code developed in Homework-6 to generate the first plot of the orbit evolution of M31 and the MW. This will help us in estimating the times at which both M31 and MW are closest to each other and when they finally merge. As we are interested in comparing the initial halo ASAM and the final merger remnant ASAM, we will calculate the halo ASAM at all the times for which the simulation files are available. We will plot the overall evolution of halo ASAM of both M31 and MW galaxies at all times, and therefore, we will be able to compare how the halo ASAM changes through a merger.

Estimating the magnitudes of spins of M31 and MW is an area of active research. Thus our simple estimates should be consistent with the current literature. For the halo merger remnant, however, multiple factors, such as the angle of collision, the relative orientation of the halo spins right before the collision, etc., will play an important role. Nonetheless, as the number of halo particles increases post-merger, the relative velocity plot (for MW and M31) shows zero velocity (but individual velocities decrease in magnitude) after galaxies have merged, and the distance between halo particles should increase due to randomization, we hypothesize that the halo remnant should have a greater spin than the individual galaxy spins before the merger.

4. RESULTS

In this paper, we quantified the evolution of halo ASAM throughout the merger of the M31 and MW galaxies. The results are plotted in Figure 3 with halo ASAM on the y-axis and time on the x-axis. The upper plot shows the halo ASAM evolution of the MW galaxy while the lower plot shows the halo ASAM evolution of the M31 galaxy. The dashed vertical lines are the periapse times calculated from the OrbitCOM code, and the last vertical line (at 6.486 Gyrs) is assumed to be the time of the final merger. As evident by the figure, the post-merger ASAM of both galaxies is higher than their initial ASAMs and seems to reach an equilibrium state.

In Figure 4, we plot the evolution of halo ASAM of MW (top panel) and M31 (middle panel) before the first periapses (at 3.957 Gyrs). In the bottom panel, we plot the halo ASAM evolution of the merger remnant. The initial ASAM (at t = 0) for MW and M31 is $-149.7\hat{i} - 35.1\hat{j} - 127.5\hat{k}$ and $-110.3\hat{i} - 116.4\hat{j} - 128.4\hat{k}$, in units of kpc-km per second. Lastly, we also calculated the time-averaged halo remnant ASAM to be $2783.4\hat{i} + 3567.2\hat{j} + 2548.9\hat{k}$. Thus, the halo merger remnant has a significantly higher ASAM than halos of both M31 and MW galaxies.

5. DISCUSSION

Our results indicate that not only do the individual galaxy halos have a higher ASAM post-merger, but their combined merger remnant as well. Exploring why the halo remnant has a higher spin than the initial haloes of MW and M31 is crucial to understand the evolution of both galaxies. To assess whether a system is bounded or not, Virial ratios can be useful: a low ratio suggests a loosely bounded system while a higher ratio suggests a tightly bounded system. Motka (2023, in prep.) found that the Virial ratio of the merger remnant of MW and M31 is slightly lower than their individual ratios, insinuating that the remnant is relatively loosely bound. As per Figure 1 (Drakos et al. 2019), a remnant that is less bound than the initial galaxies should have a higher spin. Thus, our results are not only consistent with our initial hypothesis but also with the current literature.

Furthermore, our results insinuate that the halo remnant is somehow gaining significant ASAM and orients itself in a certain direction. A possible explanation for this significantly higher ASAM of the remnant could be that angular momentum is being transferred from the orbits of MW - M31 (and M33, a satellite galaxy) into the DM halo of the remnant. Though our results are consistent with what is expected, we want to point out two uncertainties in our analysis. First, we used the original simulation files without rotating either of the galaxies into one frame. Another, more major, source of uncertainty is that while calculating the ASAM of the remnant, we simply added the individual particle angular momenta that have different frames. Though we believe that both these errors may not influence the results significantly, a more accurate approach would have been calculating the remnant ASAM from the combined center of mass frame of the remnant.

6. CONCLUSION

Investigating the rotation of dark matter halos surrounding galaxies has been an area of extensive research as it helps to comprehend both the evolution and formation of galaxies. This study focuses on exploring the average rotation of the halos encompassing the Milky Way, Andromeda, and the merger remnant of the two. The analysis of the spin evolution of the MW and M31 halos is crucial as it not only offers insight into the ultimate destiny of our galaxy but also helps us to discover the subtle physical processes that influence the merger.

Our analysis finds that the halo surrounding the merger remnant of MW and M31 has a significantly higher spin than the initial halos of both galaxies. This suggests that the halo particles of each galaxy gain angular momentum during their evolution through the merger. A possible explanation for this could be the transfer of angular momentum from the orbits of MW and M31 to the halo particles. Lastly, our results not only agree with our initial hypothesis but are also consistent with the current literature.

As an improvement, we advise future studies to quantify the ASAM evolution from a single – common – frame rather than summing the values from two different frames. Moreover, as the halo of the merger remnant is gaining significant angular momentum, it would be interesting to see how the orbital angular momentum of both galaxies compares with the final ASAM of the remnant and how the transfer of momentum happens. Including more realistic phenomena like star formation, death, and collisions would give more detailed results. Lastly, how the ASAM of the disk star particles evolves through a merger is also an enticing topic. We leave all these questions for future analyses.

ACKNOWLEDGEMENTS

We acknowledge the use of the software packages NumPy (Harris et al. 2020), SciPy (Virtanen et al. 2020), Astropy (Astropy Collaboration et al. 2013, 2018, 2022), and Matplotlib (Hunter 2007). I would also like to thank Dr. Besla for her support throughout the project and her wonderful lectures. I would also like

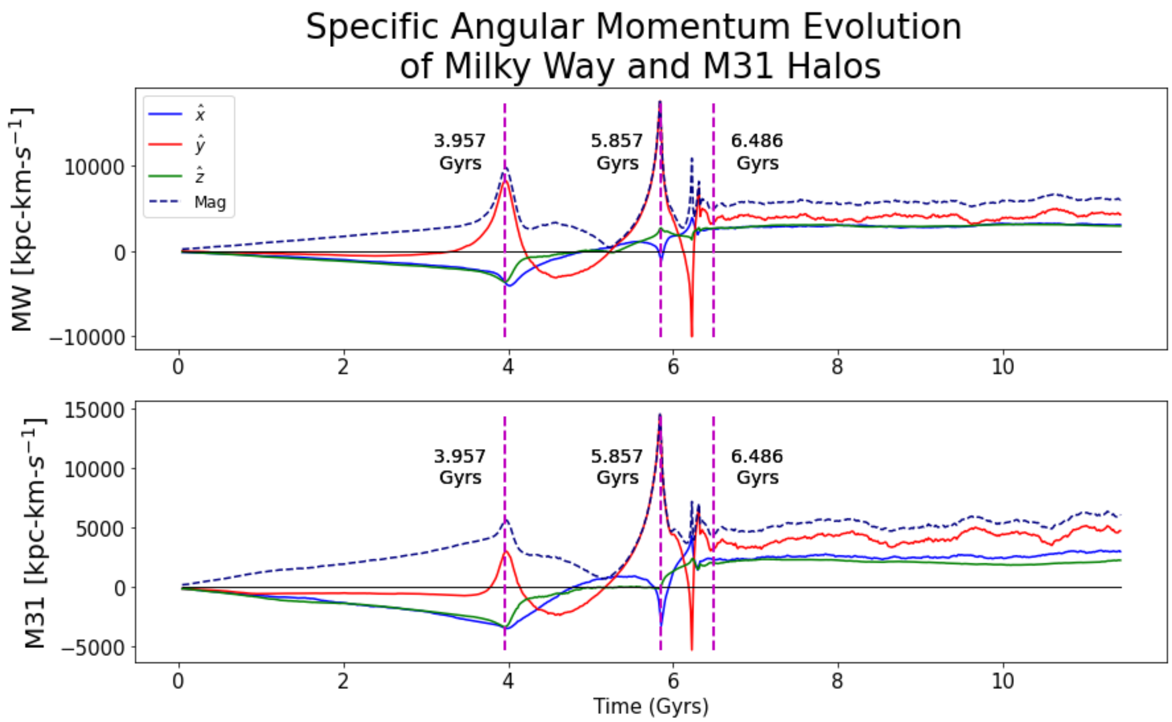

Figure 3. This figure shows the evolution of halo ASAM of MW (top) and M31 (bottom) galaxies. The y-axis is ASAM (in $kpc-km-s^{-1}$) while the x-axis is time (in Gyrs). The dashed vertical lines are periapse times. Smooth-colored tracks represent three directions while the dashed curve represents the total magnitude. Post-merger ASAM of both galaxies is higher than their initial ASAM.

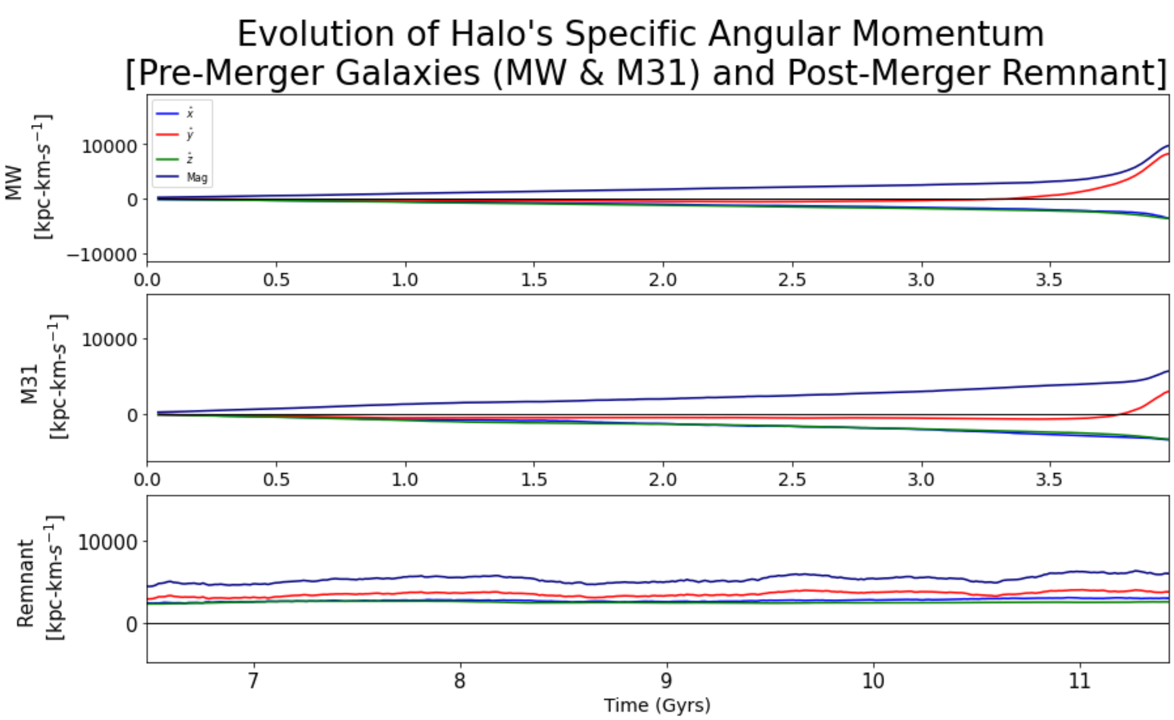

Figure 4. This figure shows the evolution of halo ASAM of MW (top) and M31 (middle) galaxies before the first periapse time and the evolution of halo remnant ASAM post-merger (bottom). The y-axis is ASAM (in $kpc - km - s^{-1}$) while the x-axis is time (in Gyrs). Colors follow the same scheme as Figure 3. ASAM of the remnant is higher than the initial ASAM of both galaxies.

to thank Hayden Foote for his help in fixing the errors in the code.

REFERENCES

Abadi, M. G., Navarro, J. F., Fardal, M., Babul, A., & Steinmetz, M. 2010, MNRAS, 407, 435, doi: 10.1111/j.1365-2966.2010.16912.x

Astropy Collaboration, Robitaille, T. P., Tollerud, E. J., et al. 2013, A&A, 558, A33, doi: 10.1051/0004-6361/201322068

Astropy Collaboration, Price-Whelan, A. M., Sipőcz, B. M., et al. 2018, AJ, 156, 123, doi: 10.3847/1538-3881/aabc4f

Astropy Collaboration, Price-Whelan, A. M., Lim, P. L., et al. 2022, apj, 935, 167, doi: 10.3847/1538-4357/ac7c74

Barnes, J., & Efstathiou, G. 1987, ApJ, 319, 575, doi: 10.1086/165480

Bett, P., Eke, V., Frenk, C. S., et al. 2007, MNRAS, 376, 215, doi: 10.1111/j.1365-2966.2007.11432.x

Bett, P., Eke, V., Frenk, C. S., Jenkins, A., & Okamoto, T. 2010, MNRAS, 404, 1137, doi: 10.1111/j.1365-2966.2010.16368.x

Bullock, J. S., Dekel, A., Kolatt, T. S., et al. 2001, Astrophys. J., 555, 240, doi: 10.1086/321477

Conselice, C. J. 2014, ARA&A, 52, 291, doi: 10.1146/annurev-astro-081913-040037

Cox, T. J., & Loeb, A. 2008, MNRAS, 386, 461, doi: 10.1111/j.1365-2966.2008.13048.x

Davis, M., Efstathiou, G., Frenk, C. S., & White, S. D. M. 1985, ApJ, 292, 371, doi: 10.1086/163168

Drakos, N. E., Taylor, J. E., Berrouet, A., Robotham, A. S. G., & Power, C. 2019, MNRAS, 487, 993, doi: 10.1093/mnras/stz1306

Fall, S. M., & Efstathiou, G. 1980, MNRAS, 193, 189, doi: 10.1093/mnras/193.2.189

Frenk, C. S., & White, S. D. M. 2012, Annalen der Physik, 524, 507, doi: 10.1002/andp.201200212

Harris, C. R., Millman, K. J., van der Walt, S. J., et al. 2020, Nature, 585, 357, doi: 10.1038/s41586-020-2649-2

Hunter, J. D. 2007, Computing in Science & Engineering, 9, 90, doi: 10.1109/MCSE.2007.55

Jiang, F., Dekel, A., Kneller, O., et al. 2019, MNRAS, 488, 4801, doi: 10.1093/mnras/stz1952

Lotz, J. M., Jonsson, P., Cox, T. J., et al. 2011, ApJ, 742, 103, doi: 10.1088/0004-637X/742/2/103

Rodriguez-Gomez, V., Sales, L. V., Genel, S., et al. 2017, MNRAS, 467, 3083, doi: 10.1093/mnras/stx305

Rubin, V. C., & Ford, W. Kent, J. 1970, ApJ, 159, 379, doi: 10.1086/150317

Shaw, L. D., Weller, J., Ostriker, J. P., & Bode, P. 2006, ApJ, 646, 815, doi: 10.1086/505016

van der Marel, R. P., Besla, G., Cox, T. J., Sohn, S. T., & Anderson, J. 2012, ApJ, 753, 9, doi: 10.1088/0004-637X/753/1/9

Virtanen, P., Gommers, R., Oliphant, T. E., et al. 2020, Nature Methods, 17, 261, doi: 10.1038/s41592-019-0686-2

Wechsler, R. H., & Tinker, J. L. 2018, ARA&A, 56, 435, doi: 10.1146/annurev-astro-081817-051756

White, S. D. M., & Rees, M. J. 1978, MNRAS, 183, 341, doi: 10.1093/mnras/183.3.341

Willman, B., & Strader, J. 2012, AJ, 144, 76, doi: 10.1088/0004-6256/144/3/76

Zwicky, F. 1933, Helvetica Physica Acta, 6, 110